Histol Histopathol (2024) 39: 1669-1683

Histology and Histopathology
From Cell Biology to Tissue Engineering

ORIGINAL ARTICLE Open Access

S100A2 upregulates GLUT1 expression to promote glycolysis in the progression of nasopharyngeal carcinoma

Ying Peng[1,2], Jing Xia[3], Dinggang Zhou[1,2], Zhongchun Yang[1,2], Ruifang Zeng[1,2], Min Xu[1,2] and Hongwei Peng[4]

[1]Department of Otolaryngology, The Affiliated Changsha Central Hospital, Hengyang Medical School, University of South China, [2]Institute of Otorhinolaryngology, Head and Neck Surgery, University of South China, Changsha, [3]ENT Teaching and Research Section, Department of Stomatology, Changsha Health Vocational College and [4]Department of Nursing, Hunan Nursing School, Changsha, Hunan, China

Summary. Nasopharyngeal carcinoma (NPC) is a malignant epithelial tumor. Among the S100 protein family members, the imbalance of S100 calcium-binding protein A2 (S100A2) was related to the pathogenesis of several types of cancer, and S100A2 has been reported to be upregulated in the plasma of NPC patients; however, its specific role in NPC pathogenesis remains unclear. Thus, this study aims to determine the potential role of S100A2 in NPC to provide novel insights into NPC management. C666-1 and NPC/HK-1 cells were transfected with S100A2 silencing/overexpression (si/oe) constructs. For *in vivo* investigations, NPC/HK-1 cells were transfected with si/oe-S100A2 to induce tumor formation in nude mice. Cellular viability and apoptosis were assessed using the CCK8 assay, colony-forming assay, and flow cytometry. Glucose uptake and lactate production levels were quantified using biochemical assays. S100A2 expression was measured via RT-qPCR, Western blot, immunohistochemistry, and immunofluorescence were performed to determine the levels of S100A2, PI3K, AKT, p-PI3K, p-AKT, GLUT1, HK-2, LDHA, and ki-67 proteins. S100A2 expression levels were significantly higher in NPC cancer tissues than in adjacent tissues. Similarly, C666-1 and NPC/HK-1 cells exhibited increased S100A2 expression, and silencing S100A2 significantly inhibited NPC cell viability, proliferation, glucose uptake, and lactate production, and induced apoptosis and decreased the protein levels of GLUT1, LDHA, and HK2 in NPC cells. Conversely, S100A2 overexpression enhanced these characteristics in NPC cells but could be mitigated by the PI3K/AKT inhibitor (LY294002). Silencing S100A2 suppressed the tumor formation of NPC/HK-1 cells, while S100A2 overexpression promoted tumor formation and could be hindered by a GLUT1 inhibitor (WZB117). S100A2 is upregulated in cancer tissues of NPC patients and was found to promote proliferation, glycolysis, and tumor formation in NPC cells through its interaction with GLUT1.

Key words: Nasopharyngeal carcinoma, S100A9, GLUT1, Glycolysis, PI3K/AKT

Corresponding Author: Hongwei Peng, Department of Nursing, Hunan Nursing School, Changsha 410318, Hunan, PR China. e-mail: pzc0731@163.com

www.hh.um.es. DOI: 10.14670/HH-18-778

Introduction

The epidemiology of nasopharyngeal carcinoma (NPC) has long been fascinating due to its distinct geographic distribution patterns (Chang et al., 2021). NPC is categorized as a malignant epithelial tumor with a significantly high incidence in North Africa and Southeast Asia (Tang et al., 2021). At present, concurrent chemoradiotherapy is the standard treatment for stage II NPC. However, it only achieves a three-year non-failure survival rate in low-risk NPC patients (Tang et al., 2022). Although it is a highly prevalent cancer affecting the head and neck region, its exact etiology remains unclear, and effective personalized therapeutic approaches are lacking (Ding et al., 2021). Therefore, exploring oncogenes and potential mechanisms associated with NPC development may offer valuable insights for its treatment.

Clinical research revealed that S100 calcium-binding protein P (S100P) is upregulated in 45 of 78 (57.7%) NPC patients but only upregulated in 5 of 30 (16.7%) benign inflammation patients (Liu et al., 2017). Histopathological examination has demonstrated moderate expression of S100 in poorly differentiated nasopharyngeal papillary adenocarcinoma (Huang et al.,

2019). In addition, the S100P protein is a subtype of the S100 protein family, and its interaction with RAGE was found to enhance the migration and proliferation potential of C666-1 cells (Wang et al., 2021a). Members of the S100 calcium-binding protein family have been commonly involved in the development process of NPC, such as S100A14 (Meng et al., 2020), S100A6 (Li et al., 2017), S100A4 (Lin et al., 2016), S100A1 (Chen et al., 2018), S100A8, and S100A9 (Yan et al., 2015; Hu et al., 2021). Among the S100 protein family, S100 calcium-binding protein A2 (S100A2) has been confirmed to be present in malignant tumors and inflammatory diseases (Sugino and Sawada, 2022). ELISA analysis has further validated elevated plasma levels of S100A2 in NPC patients (Lin et al., 2013). Utilizing proteomic data and subsequent western blot validation, it has been established that S100A2 is upregulated in the squamous cells of nasopharyngeal cancer (Feng et al., 2011). However, the specific role of S100A2 in NPC remains to be elucidated.

It is well-established that cancer cells prefer glycolysis to support their proliferation (Oyang et al., 2023). SETD1A overexpression positively regulates cell proliferation and induces aerobic glycolysis in NPC cells through the PI3K/AKT pathway *in vitro* (Huang et al., 2022). Similarly, in colorectal cancer, S100A2 activates the PI3K/AKT pathway, upregulates GLUT1 expression, induces glycolytic reprogramming, and promotes cell proliferation (Li et al., 2020). Furthermore, elevated GLUT1 levels have been observed in nasopharyngeal tissues of NPC patients, correlating with clinical staging and lymph node metastasis (Zhou et al., 2017). Based on these insights, our hypothesis posits that S100A2 may participate in glycolysis and proliferation processes in NPC, potentially via its interaction with GLUT1. This study aims to validate the role of S100A2 in glycolysis and proliferation in NPC, offering new perspectives for NPC treatment.

Materials and methods

Clinical samples and S100A2 expression analysis

This study was approved by the Medical Ethics Committee of Changsha Central Hospital (No. 2021006). Tumor (NPC) and paratumoral tissue (Non-NPC) samples from six NPC individuals were obtained from the hospital, with six cases in each group, and histopathological examination was conducted to confirm the diagnosis of all collected specimens, following which they were used for the assessment and analysis of S100A2 protein expression.

NPC is a highly prevalent malignant head and neck tumor (Cantù, 2023). Based on the analysis of the cancer genome atlas (TCGA) database (https://www.cancer.gov/ccg/research/genome-sequencing/tcga)(Carrot-Zhang et al., 2020), S100A2 expression in the Normal and Tumor groups of head and neck cancer was determined by the Wilcoxon test.

Cell experiments and processing

The NP69 (JY291) immortalized nasopharyngeal epithelial cell line (Shanghai Jinyuan Biotech Co., Ltd., Shanghai, China) was cultured in KM medium, while the C666-1 (AW-CCH168, Abiowell, Changsha, China) and NPC/HK-1 (AW-CCH310, Abiowell, Changsha, China) cell lines were incubated in Roswell Park Memorial Institute (RPMI) 1640 medium supplemented with 10% fetal bovine serum (FBS) and 1% Penicillin-Streptomycin. All cells were maintained at 37°C, 95% air, and 5% CO_2.

To investigate S100A2 expression, the cells were divided into three groups: NP69, C666-1, and NPC/HK-1. To explore the functional role of S100A2 in NPC cells, C666-1 and NPC/HK-1 cells were further categorized into the following silencing/overexpression (si/oe) experimental groups: si-NC, si-S100A2#1, si-S100A2#2, oe-NC, oe-S100A2, LY294002, and oe-S100A2+LY294002. Transfection was performed first in the transfection group before any subsequent treatments. Additionally, cells in the LY294002 group were treated with LY294002 (10 μM), a PI3K inhibitor (CAS No.: 154447-36-6, MCE, New Jersey, USA), for 48 hours (Huang et al., 2022).

Cell transfection

For lentivirus transfection, approximately 2×10^5 cells/well. On the next day, the initial medium was replaced with 0.5 mL of fresh medium containing 10 μg/mL polybrene. Subsequently, 10 μL of 1×10^8 TU/mL S100A2 overexpression/interference lentivirus suspension (HonorGene, Changsha, China) was added. After an incubation period, the medium was refreshed. GFP expression was assessed using a fluorescence microscope after 72 hours of infection. The cells were then subjected to antibiotic selection in a culture medium (approximately one week) to isolate successfully transfected cells. The selected cells underwent further purification through a limiting dilution method and were subsequently expanded in culture after purification (Lin et al., 2021). Once a sufficient cell number was attained, cells were harvested, and RNA was extracted for RT-PCR validation of S100A2 expression. Cells testing positive were suitable for further experiments or could be stored frozen until subsequent use. N=3 replications/group.

The overexpression plasmid for the human *S100A2* gene, pcDNA3.1-S100A2-3xFlag, was procured commercially from HonorGene (Changsha, China). This plasmid was designed with the following sequences: F - CACTAGTCCAGTGTGGTGGAATTCGCCACCATGATGTGCAGTTCTCTGGAGC and R - GTCGAAGGGCCCTCTAGACTCGAGGGGTCGGTCTGGGCAGCCCTG. Additionally, pHG-S100A2-sh1 (CACTGTCATGTGCAATGACTT) and pHG-S100A2-sh2 (CGACAAGTTCAAGCTGAGTAA) interference plasmids were also commercially obtained from HonorGene

(Changsha, China). All of these expressing plasmids underwent thorough verification by sequencing. N=3 replications/group.

Cell counting Kit-8 (CCK8)

Cells (2×10^4 cells/well) were cultured in 24-well plates, with each well containing 300 μL of cell suspension. Each experimental group consisted of three replicate wells. Subsequently, 30 μL of CCK8 reagent (NU679, Toren, Japan) was added to each well. The plates were then incubated at 37°C in an atmosphere of 5% CO_2 for 4 hours. To quantify cell viability, the absorbance at 450 nm was measured using a microplate reader (MB-530, HEALES, Shenzhen, China), and the average values were utilized to construct a bar graph.

Biochemical testing

The levels of glucose and lactate in the cell supernatant were quantified using glucose (A154-1-1, NJJCBIO, Nanjing, China) and lactate (A019-2-1, NJJCBIO, Nanjing, China) detection kits, using an enzyme-labeled instrument and a visible light spectrophotometer to determine glucose residue and lactate production. N=3 replications/group.

Colony-forming assay

Cells from different experimental groups were harvested during their exponential growth phase and digested by trypsin (0.25%), dispersed into single cells through pipetting, and resuspended in a complete culture medium containing 10% FBS. Then, 200 cells were taken from each group and seeded into a 6-well plate with 1 mL of medium at room temperature. The plates were gently swirled to evenly disperse the cells and placed in the cell culture incubator with appropriate periodic medium changes. When visible clones appeared in the culture dish, the culture was terminated, the culture medium was discarded, the cells were carefully washed twice with PBS solution, 1 mL of 4% paraformaldehyde was added to each well for a 15-minute fixation, and 1 mL of staining working solution was applied and kept at 37°C for 30 min. The staining solution was washed away using running water, and a mobile phone was used to take photos of the cells for observation. N=3 replications/group.

Apoptosis

The cells were suspended in 500 μL of Binding buffer, followed by adding 5 μL of Annexin V-APC (KGA1007, KeyGen Biologicals, Jiangsu, China) and 5 μL of Propidium Iodide. The mixture was thoroughly mixed and incubated at 37°C without light for 10 min. Afterward, the cells were washed once with PBS and subjected to measurement using a flow cytometer. N=3 replications/group.

Immunofluorescence (IF)

Cell slides were washed 2-3 times with PBS, fixed with 4% paraformaldehyde for 30 min, and then rinsed three times with PBS for 5 min each time. Afterward, the slides were treated with 0.3% Triton X-100 and incubated for 30 min at 37°C. Subsequent blocking was performed using 5% BSA at 37°C for 60 min. The slides were then incubated overnight at 4°C with anti ti-GLUT1 (ab115730, 1:50, Abcam, UK) and anti-S100A2 (bsm-51330m, 1:50, Bioss, USA) antibodies. Following primary antibody incubation, the slides were exposed to 100 μL of goat anti-rabbit IgG (H+L) secondary antibody, Alexa Fluor488 (AWS0005c, 1:200, Abiowell, Changsha, China), and Goat anti-Mouse IgG (H+L) Secondary Antibody, Alexa Fluor594 (AWS0004c, 1:200, Abiowell, Changsha, China), for 90 min at 37°C. Subsequently, the slides were stained with DAPI solution for 10 min at 37°C, rinsed with PBS for 5 min, and finally mounted with glycerol buffer for analysis using a fluorescence microscope (BA210T, Motic, Xiamen, China). N=3 replications/group.

Tumorigenesis in nude mice

A total of 12 BALB/c mice (four weeks old) were bought from Hunan Slack Jinda Laboratory Animal Co., Ltd., and divided into four groups: control, si-S100A2, oe-S100A2, and oe-S100A2+WZB117. Stable transfection with si-S100A2 or oe-S100A2 of NPC/HK-1 cells (5×10^6) was injected into the subcutaneous tissue on the right side of the nude mice. NPC/HK-1 cells in the control group were transfected with oe-NC and si-NC cells. Before the start of treatment, the average tumor volume had grown to 130 mm^3. WZB117 intervention was administered at 20 mg/kg/day by intraperitoneal injection (Shibuya et al., 2015). Tumor volume was assessed every other day using calipers. After 28 days, mice were humanely euthanized using CO_2 inhalation, and their tumor tissues were harvested for subsequent analyses. All experimental procedures and animal care were conducted in accordance with the approval of the Animal Care and Use Committee of Changsha Central Hospital (Approval No. 2021006), which is affiliated with the University of South China.

RT-qPCR

Total RNA was isolated using Trizol, and the concentration was determined using a UV spectrophotometer at 260~280 nm. Primers were synthesized by the Beijing Genomics Institute. For S100A2, the primer sequences were: F - CACGACACCTCCCACTTCC and R - TGCCATTCCCACTCATTCCC (141bp, http://www.ncbi.nlm.nih.gov/gene/6273). For β-actin, the primer sequences were: F - ACCCTGAAGTACCCCATCGAG and R - AGCACAGCCTGGATAGCAAC (224 bp, https://www.ncbi.nlm.nih.gov/gene/60). cDNA was generated by reverse transcription of the total mRNA

using the mRNA kit (CW2569, CWBIO, Beijing, China). The amplification reactions were performed using the UltraSYBR Mixture kit (CW2601, CWBIO, Beijing, China) and a real-time PCR machine (PIKOREAL96, Thermo, Massachusetts, USA). The amplification program consisted of an initial denaturation at 95°C for 10 min, followed by 40 cycles of denaturation at 95°C for 10 seconds, and annealing/extension at 60°C for 30 seconds. The relative expression levels of the target gene were determined using the $2^{-\Delta\Delta Ct}$ method in each group.

Western blot

After the experiment, the cell samples and tumor tissues were collected, and a lysis buffer (RIPA, AWB0136, Abiowell, Changsha, China) was added to extract total protein. BCA was used to analyze protein levels. The protein sample was separated using SDS-PAGE. The proteins were transferred onto a polyvinylidene fluoride membrane using a transmembrane electrophoresis apparatus (AWC0114, Abiowell, Changsha, China). Then, the membranes were incubated with the first antibody (Table 1) at 4°C overnight. Afterward, the membranes were incubated with anti-IgG (SA00001-1/2, 1:5000/6000, Proteintech, Chicago, USA) for 90 min at 37°C, visualized using a chemiluminescence assay (AWB0005, Abiowell, Changsha, China) and analyzed using ChemiScope6100 software (CLiNX, Shanghai, China).

Table 1. Antibody information.

Protein	Item	Ratio	Weight	Time	Source
S100A2	AWA44768	1:1000	10KDa	30 min	Abiowell
GLUT1	AWA43436	1:1000	55KDa	30 min	Abiowell
HK2	AWA02524	1:1000	102KDa	120 min	Abiowell
LDHA	AWA42156	1:1000	36KDa	60 min	Abiowell
P-PI3K	AWA40427	1:10000	85KDa	110 min	Abiowell
PI3K	AWA40428	1:10000	85KDa	110 min	Abiowell
p-AKT	AWA00626	1:1000	56KDa	80 min	Abiowell
AKT	AWA00628	1:1000	56KDa	80 min	Abiowell
β-actin	AWA80002	1:5000	42KDa	60 min	Abiowell

Immunohistochemistry

Tumor tissues were sectioned into 5 μm slices, followed by a 12-hour bake at 60°C. The sections underwent a series of treatments: three immersions in xylene for 20 min each, sequential exposure to 100%, 100%, 95%, 85%, and 75% ethanol for 5 min at each step, and heating in citrate buffer (0.01 M, pH=6.0) with a 20-minute boil. After cooling to 37°C, the sections were washed with 0.01 M PBS (pH=7.2~7.6) for 3 min and repeated three times. Subsequently, sections were treated with 1% periodic acid at 37°C for 10 min, followed by PBS rinses for 3 min, repeated three times. The primary antibody ki67 (1:200, AWA10320,

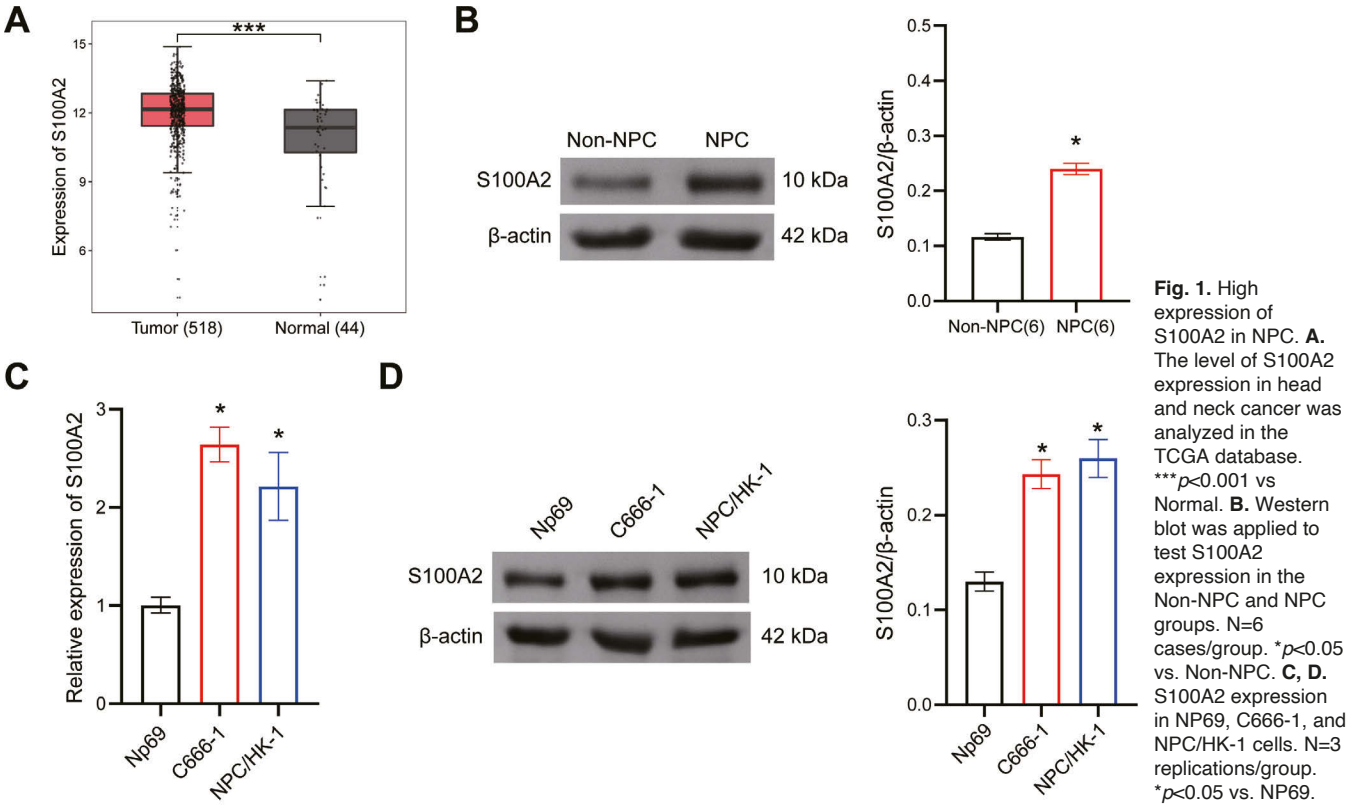

Fig. 1. High expression of S100A2 in NPC. **A.** The level of S100A2 expression in head and neck cancer was analyzed in the TCGA database. ***p<0.001 vs Normal. **B.** Western blot was applied to test S100A2 expression in the Non-NPC and NPC groups. N=6 cases/group. *p<0.05 vs. Non-NPC. **C, D.** S100A2 expression in NP69, C666-1, and NPC/HK-1 cells. N=3 replications/group. *p<0.05 vs. NP69.

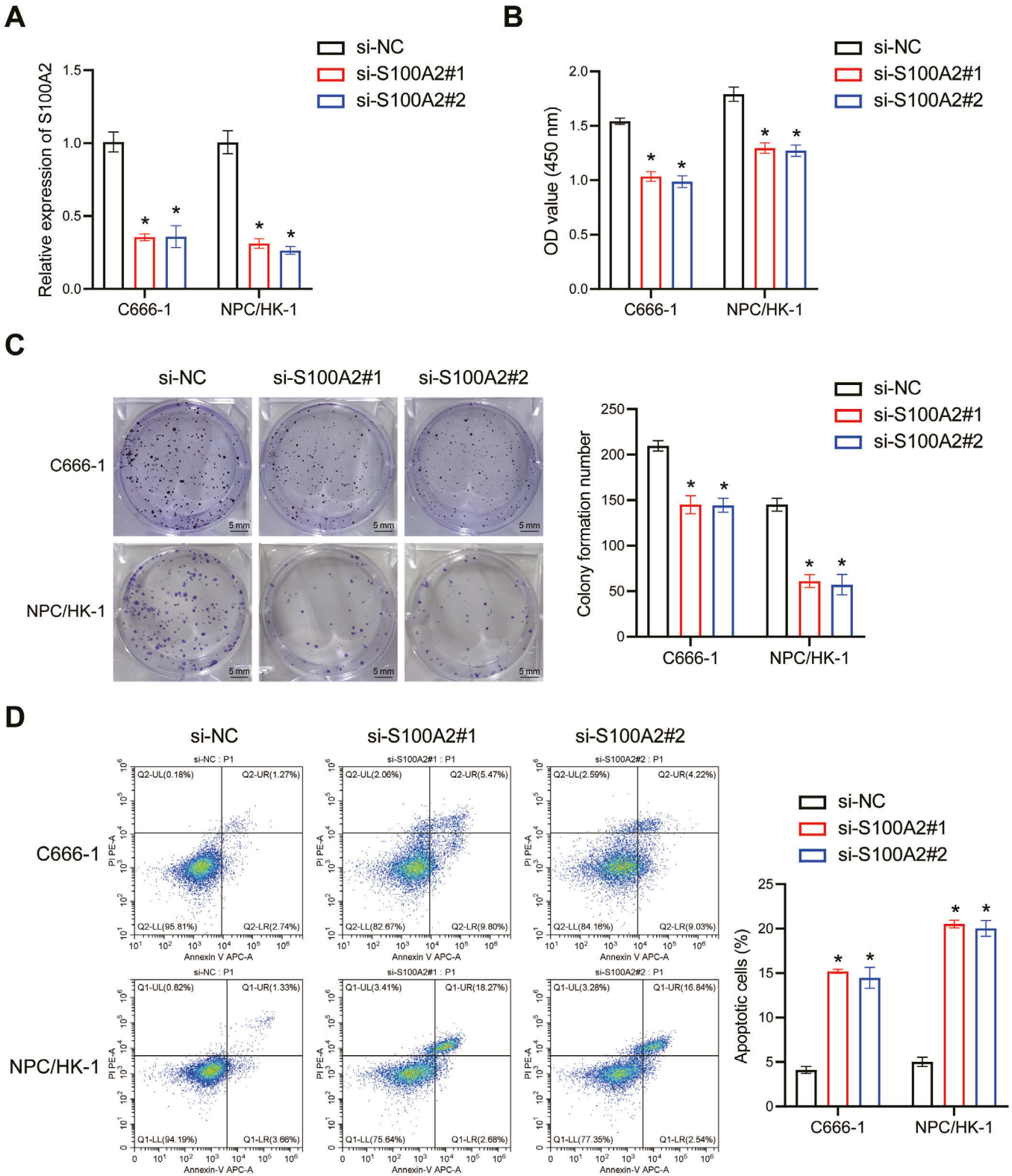

Fig. 2. Silencing S100A2 in NPC cells inhibited cell proliferation and glycolysis. **A.** RT-qPCR detection of S100A2 mRNA. **B.** CCK8 of cell viability. **C.** Colony-forming assay of cell proliferation (5 mm). **D.** Flow cytometry was applied to detect cell apoptosis. N=3 replications/group. *p<0.05 vs. si-NC.

Abiowell, Changsha, China) was applied dropwise and incubated overnight at 4°C. The sections were then exposed to 100 μL of IgG antibody-HRP conjugate and incubated at 37°C for 30 min. A pre-made DAB solution was added dropwise and incubated at 37°C for 1-5 min. After a 10-minute counterstaining with hematoxylin, sections were rinsed with water and blued with PBS. Dehydration followed with an alcohol gradient (60-100%), each step lasting 5 min. Sections were treated with xylene for 10 min, sealed with neutral resin, and observed under a microscope (BA410T, Xiamen, Motic). Image analysis was conducted using Image-Pro-Plus.

Statistical analysis

Statistical analysis was performed using Prism 8.0 software (Graphpad, San Diego, USA). Data are presented as mean ± standard deviation. First, tests for normality and homogeneity of variance were performed. If the data met the conditions of normality and homogeneity of variance, a non-paired t-test was applied for intergroup comparisons. One-way analysis of variance (ANOVA) or repeated measures ANOVA was applied for comparisons in multiple groups with Tukey's *post-hoc* test. $p<0.05$ was determined statistically significant.

Results

High expression of S100A2 in NPC

TCGA analysis showed a significant upregulation of S100A2 in head and neck cancer tissues (Fig. 1A). To further investigate the expression of S100A2 in NPC, we collected samples from NPC patients, including cancer tissues and adjacent tissues (six cases/group). The analysis revealed a significant upregulation of S100A2 expression in the NPC group with to the Non-NPC group (Fig. 1B). Further validation using NPC cell lines demonstrated that both S100A2 mRNA and protein levels were notably increased in C666-1 and NPC/HK-1 cells compared with NP69 cells (Fig. 1C,D). These findings confirm the upregulation of S100A2 in both NPC cells and tissues, suggesting its potential as a target for further investigation.

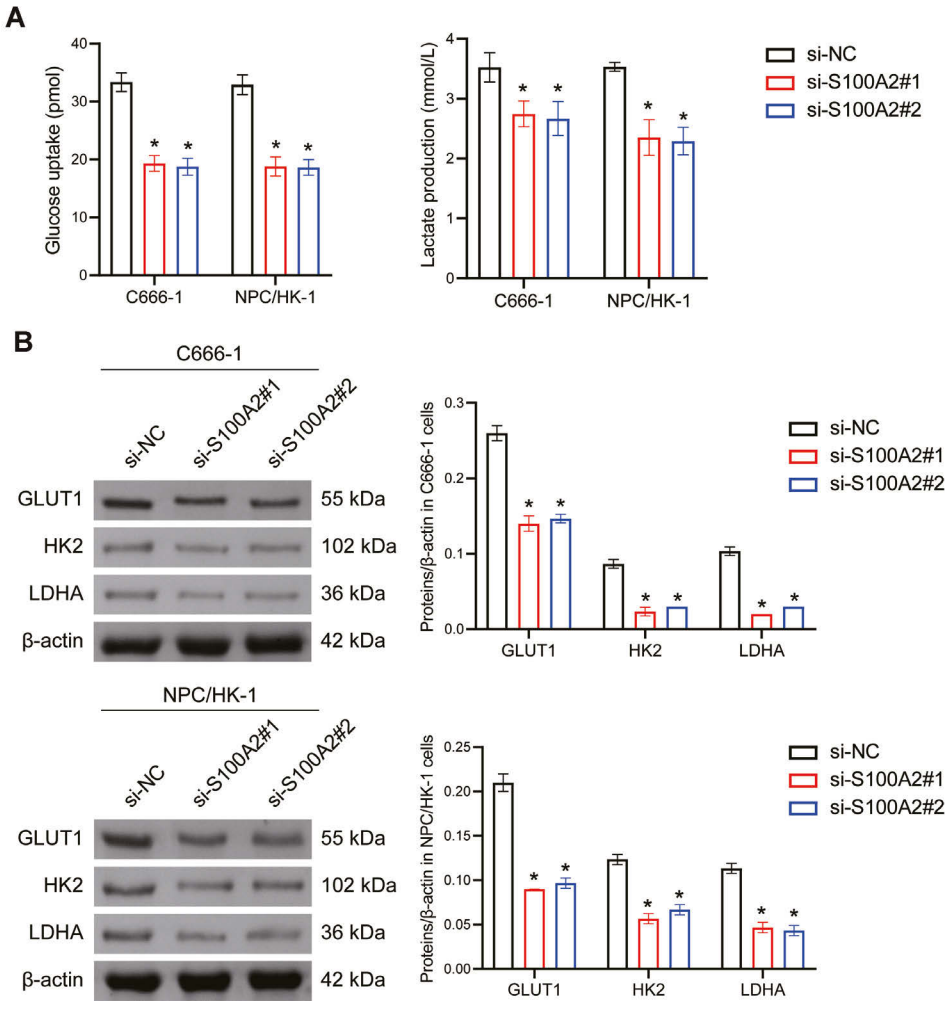

Fig. 3. Silencing S100A2 in NPC cells inhibited cell proliferation and glycolysis. **A.** Biochemical method to detect glucose uptake and lactate production levels in cells. **B.** The level of GLUT1, HK2, and LDHA proteins was detected by western blot in NPC cells. N=3 replications/group. *$p<0.05$ vs. si-NC.

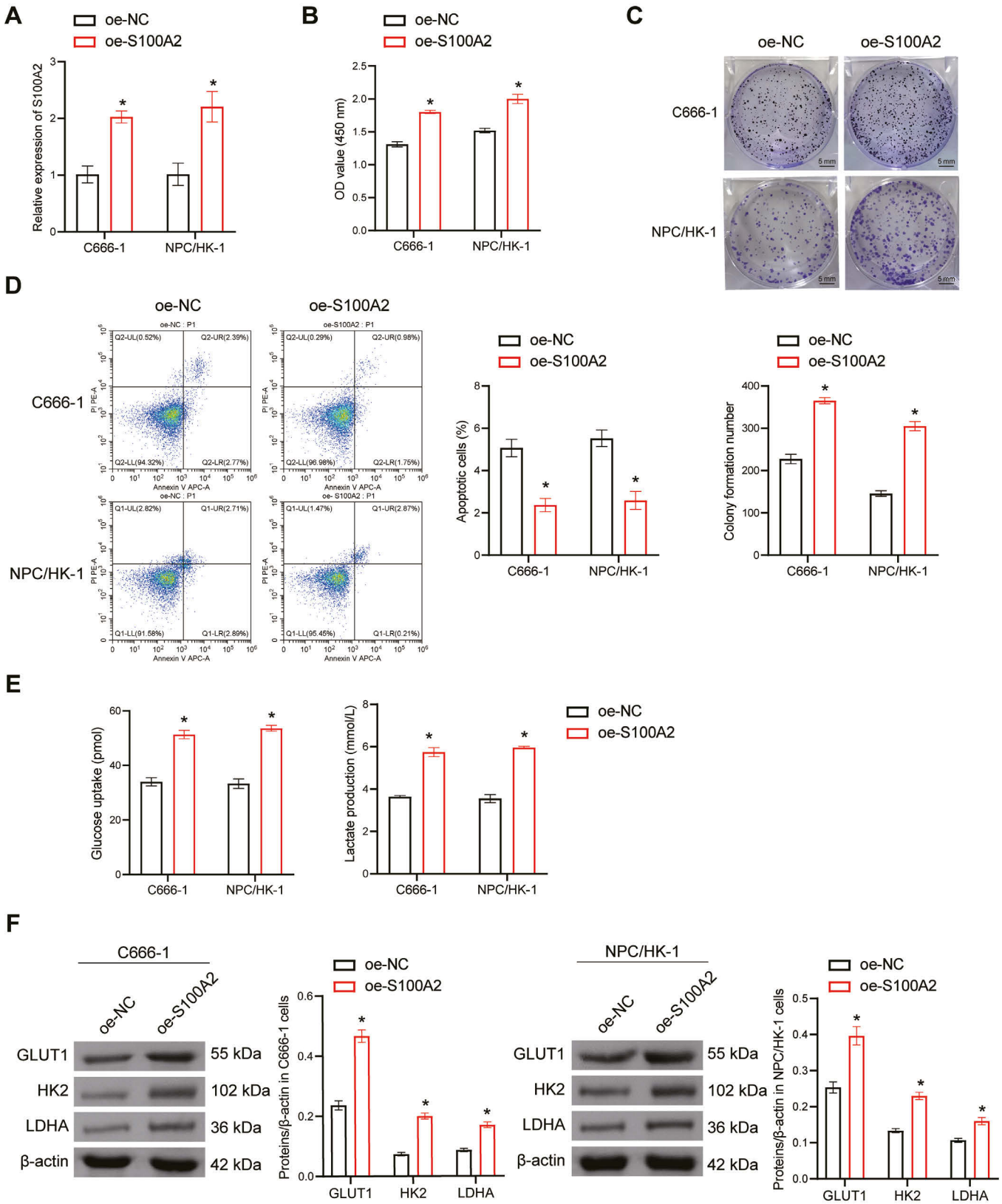

Fig. 4. Overexpression of S100A2 in NPC cells promoted viability and glycolysis. **A.** RT-qPCR was applied to test the expression of S100A2. **B.** CCK8 assay of cell viability. **C.** Colony-forming assay (5 mm). **D.** Flow cytometry was applied to detect cell apoptosis. **E.** Glucose uptake and lactate production levels in cells. **F.** Western blot was applied to detect the level of GLUT1, HK2, and LDHA proteins in cells. N=3 replications/group. *p<0.05 vs. oe-NC.

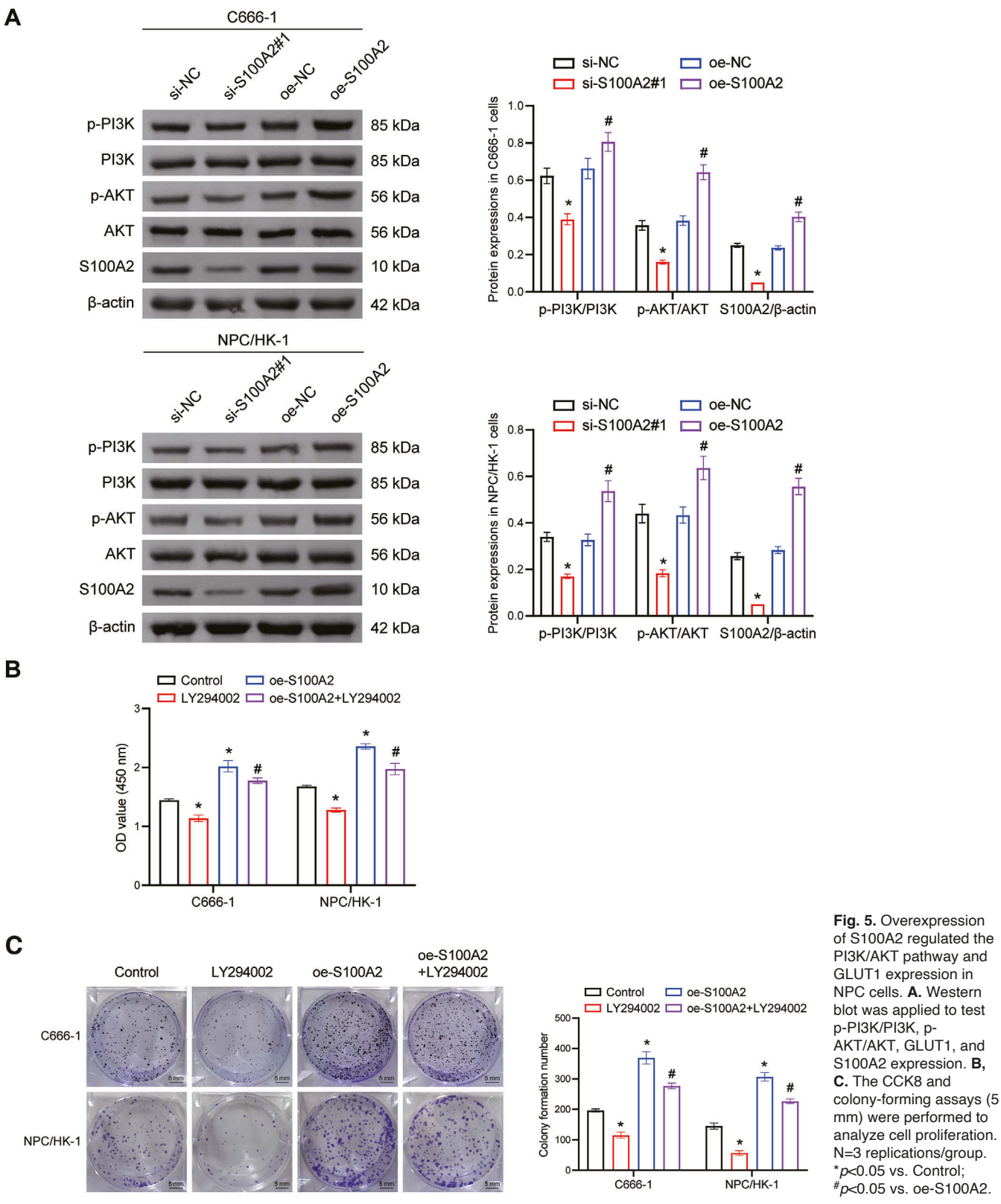

Fig. 5. Overexpression of S100A2 regulated the PI3K/AKT pathway and GLUT1 expression in NPC cells. **A.** Western blot was applied to test p-PI3K/PI3K, p-AKT/AKT, GLUT1, and S100A2 expression. **B, C.** The CCK8 and colony-forming assays (5 mm) were performed to analyze cell proliferation. N=3 replications/group. **p*<0.05 vs. Control; #*p*<0.05 vs. oe-S100A2.

Silencing S100A2 inhibited the viability and glycolysis of NPC cells

To investigate the action of S100A2 in NPC cells, C666-1 and NPC/HK-1 cells were transfected with si-S100A2. The S100A2 mRNA levels were significantly reduced in both the si-S100A2#1 and si-S100A2#2 groups compared with the si-NC group, confirming the successful generation of NPC cells with silenced S100A2 (Fig. 2A). Furthermore, silencing S100A2 suppressed cell viability and proliferation in NPC cells (Fig. 2B,C). Notably, it also promoted apoptosis in NPC cells (Fig. 2D). Moreover, biochemical assessments revealed that silencing S100A2 in NPC cells reduced glucose uptake and lactate production (Fig. 3A). Subsequent tests indicated that silencing S100A2 downregulated the expression of GLUT1, LDHA, and HK2 proteins in NPC cells (Fig. 3B). Collectively, these findings provide evidence that silencing S100A2 hinders both proliferation and glycolytic processes in NPC cells.

Overexpression of S100A2 promoted proliferation and glycolysis in NPC cells

Further studies were conducted to investigate the action of S100A2 overexpression in NPC cells by using oe-S100A2. Compared with the oe-NC group, S100A2 expression was significantly elevated in the oe-S100A2 group, confirming the successful construction of S100A2 overexpression in the NPC cell line (Fig. 4A). Additionally, overexpression of S100A2 in NPC cells promoted viability and proliferation (Fig. 4B,C) and also inhibited apoptosis (Fig. 4D). Furthermore, biochemical testing showed that overexpression of S100A2 promoted glucose uptake and lactate production in NPC cells (Fig. 4E). Overexpression of S100A2 promoted GLUT1, HK2, and LDHA protein levels in NPC cells (Fig. 4F). These results demonstrated that overexpression of S100A2 enhanced proliferation and the glycolysis process in NPC cells.

PI3K/AKT signaling mediated the co-expression of S100A2 and GLUT1 in NPC cells

To investigate the involvement of the PI3K/AKT signaling pathway in the regulatory effects of S100A2 on NPC cells, western blot analysis was employed to assess protein levels in the PI3K/AKT pathway. Silencing S100A2 in NPC cells reduced the levels of p-PI3K/PI3K, p-AKT/AKT, and S100A2 proteins (Fig. 5A). Conversely, overexpression of S100A2 in NPC cells increased p-PI3K/PI3K, p-AKT/AKT, and S100A2

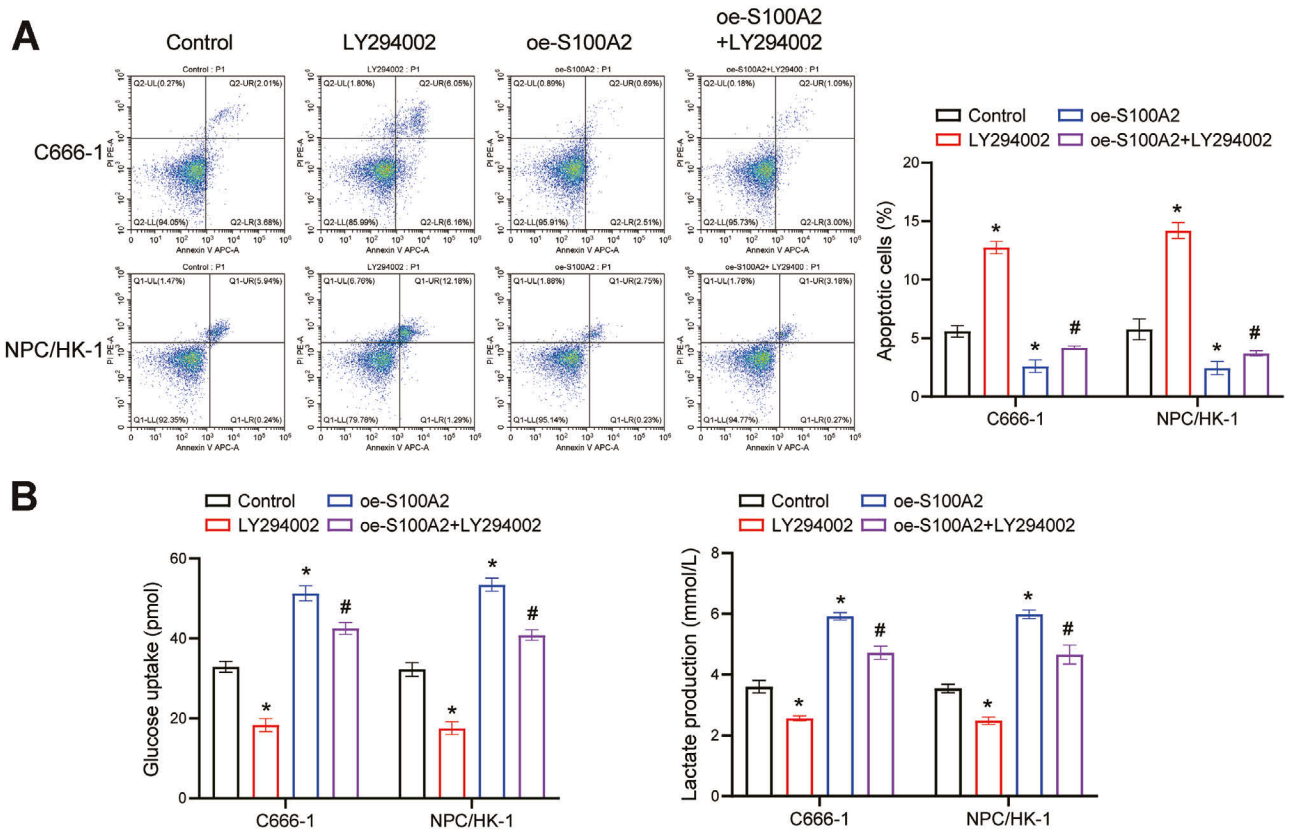

Fig. 6. Overexpression of S100A2 regulated the PI3K/AKT pathway and GLUT1 expression in NPC cells. **A.** Cell apoptosis was measured by flow cytometry. **B.** Glucose uptake and lactate production levels in the cells. N=3 replications/group. *p<0.05 vs. Control; $^{\#}p$<0.05 vs. oe-S100A2.

levels (Fig. 5A). Subsequent intervention experiments using LY294002 revealed that it inhibited the viability and proliferation of both NPC cells and S100A2-overexpressing NPC cells and induced apoptosis in both groups (Figs. 5B-C, 6A). Biochemical analysis demonstrated that LY294002 suppressed glucose uptake and lactate production in both NPC cells and S100A2-overexpressing NPC cells (Fig. 6B). Furthermore, LY294002 inhibited the activation of the PI3K/AKT pathway, while it did not affect S100A2 expression in either NPC cells or S100A2-overexpressing NPC cells (Fig. 7). Immunofluorescence co-localization studies showed that LY294002 inhibited the expression of GLUT1 proteins, while it did not affect the expression of S100A2 in either NPC cells or S100A2-overexpressing NPC cells (Fig. 8). These results collectively indicate that the PI3K/AKT signaling pathway mediates the colocalization of S100A2 and GLUT1 in NPC cells and represents a crucial pathway regulated by S100A2 in NPC.

Overexpression of S100A2 promoted NPC tumor formation by upregulating GLUT1 expression

The role of S100A2/GLUT1-related glycolysis in NPC tumor formation was determined using nude mice. Comparative analysis revealed that silencing S100A2 significantly inhibited tumor volume compared with the Control group (Fig. 9A). Conversely, S100A2 overexpression promoted tumor volume at each time point (Fig. 9A). Interestingly, in nude mice with overexpressed S100A2 NPC cell tumors, treatment with WZB117 led to a significant reduction in tumor volume at each time point (Fig. 9A). Observations and weight analysis of tumors demonstrated that silencing S100A2 reduced tumor weight at 28 days (Fig. 9B,C). Furthermore, treatment with WZB117 reduced the tumor weight in the group of NPC cells overexpressing S100A2 at 28 days (Fig. 9B,C). Immunohistochemistry analysis confirmed that silencing S100A2 resulted in a decrease in the level of Ki-67 in tumor tissues (Fig. 9D). Treatment with WZB117 also reduced the expression of Ki-67 in the group of NPC cells overexpressing S100A2 tumors (Fig. 9D). Western blotting further validated that silencing S100A2 inhibited GLUT1 expression in tumor tissues (Fig. 9E). Overexpression of S100A2, on the other hand, promoted GLUT1 expression in tumors, however, this effect was blocked by WZB117 (Fig. 9E). Overall, S100A2 was found to promote the proliferation and glycolysis of NPC tumors through GLUT1 (Fig. 9F). These findings indicate that overexpression of S100A2 promotes the formation of NPC tumors, which WZB117, a GLUT1 inhibitor, can effectively block.

Discussion

In endometrial cancer, a high expression of S100A2 was associated with shorter survival and disease-specific

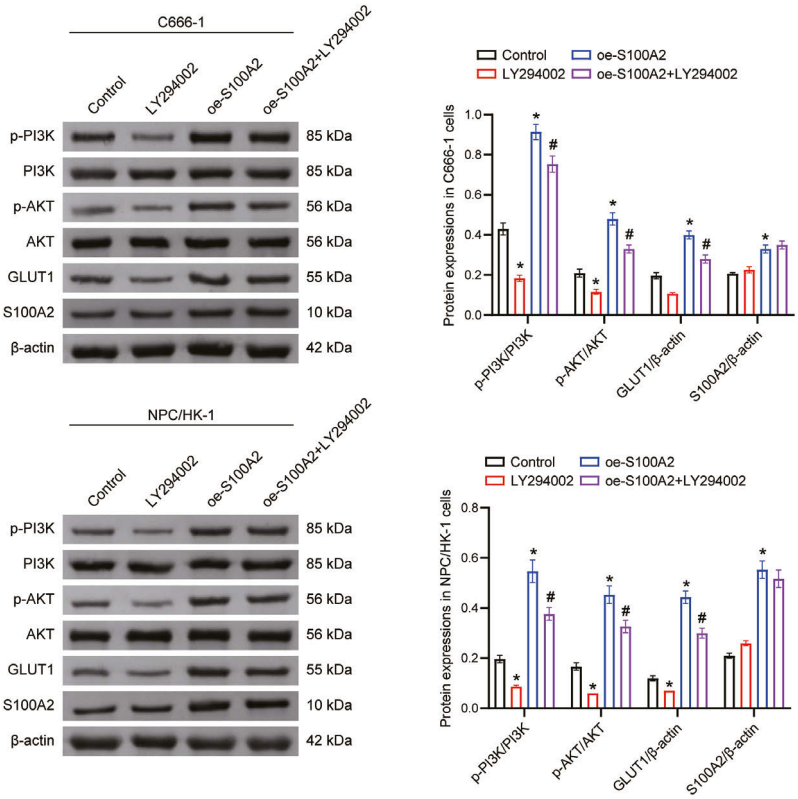

Fig. 7. The PI3K/AKT pathway mediated co-expression of S100A2 and GLUT1 in NPC cells. The protein expression of p-PI3K/PI3K, p-AKT/AKT, GLUT1, and S100A2 were assessed by western blot. S100A2 (25 μm). N=3 replications/group. *p<0.05 vs. Control; $^{\#}p$<0.05 vs. oe-S100A2.

survival compared with low S100A2 expression (Zhang et al., 2022). In addition, low S100A2 expression signals suggested a good prognosis for patients with colorectal cancer (Yang et al., 2023). S100A2 was found to be over-expressed in advanced non-small cell lung cancer (Wang et al., 2021b). Comparatively, the results of our present study showed that S100A2 expression in the cancerous tissue of NPC patients was highly expressed compared with adjacent normal tissues, and it was highly expressed in C666-1 and NPC/HK-1 cells. However, the clinical significance of S100A2 in NPC still needs further investigation, and these studies demonstrate that S100A2 is one of the potential targets for the treatment of NPC within the S100 protein family.

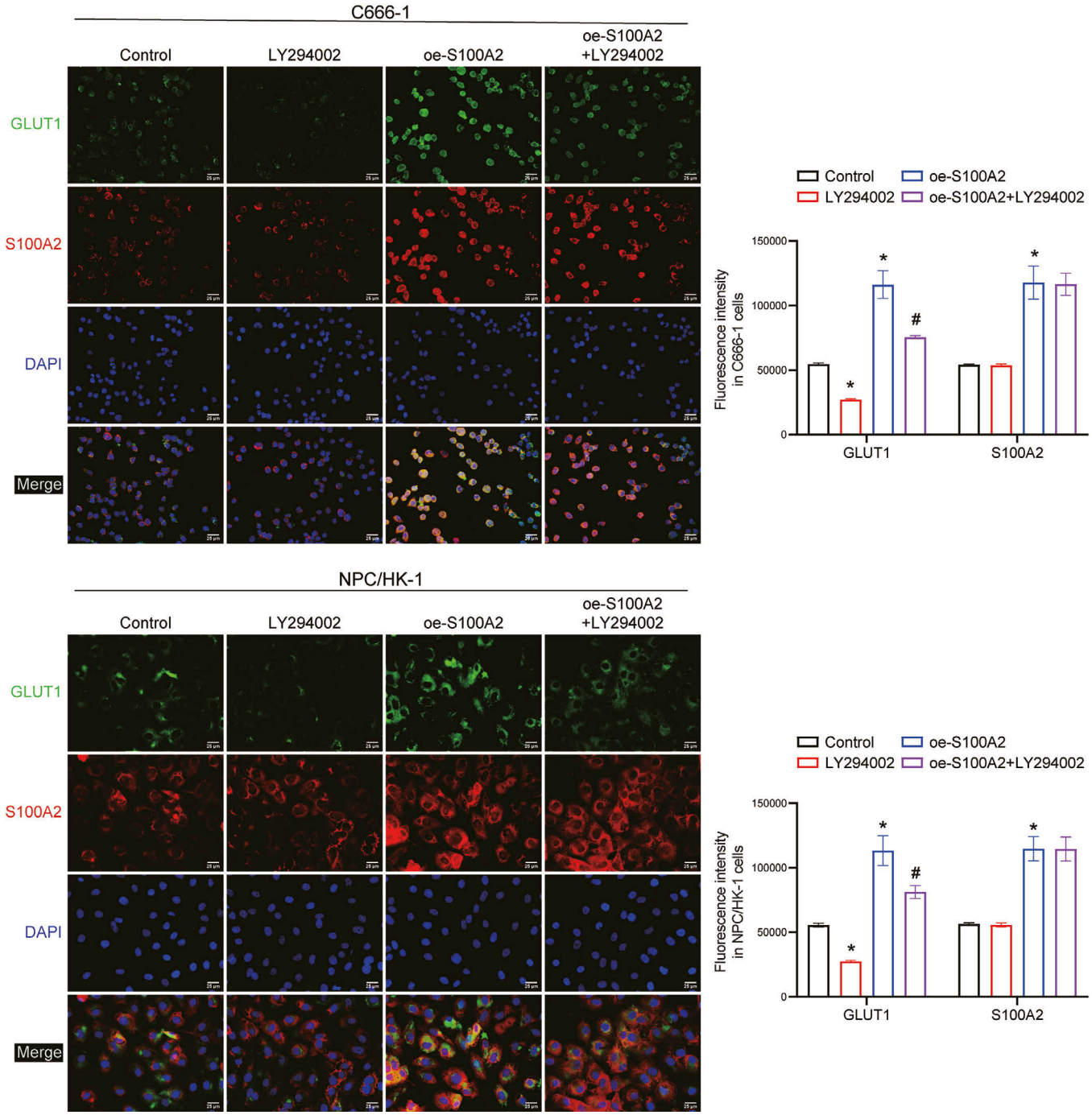

Fig. 8. The PI3K/AKT pathway mediated co-expression of S100A2 and GLUT1 in NPC cells. Immunofluorescence double staining was performed to test the positivity of GLUT1 and S100A2 (25 μm). N=3 replications/group. *p<0.05 vs. Control; $^{\#}p$<0.05 vs. oe-S100A2.

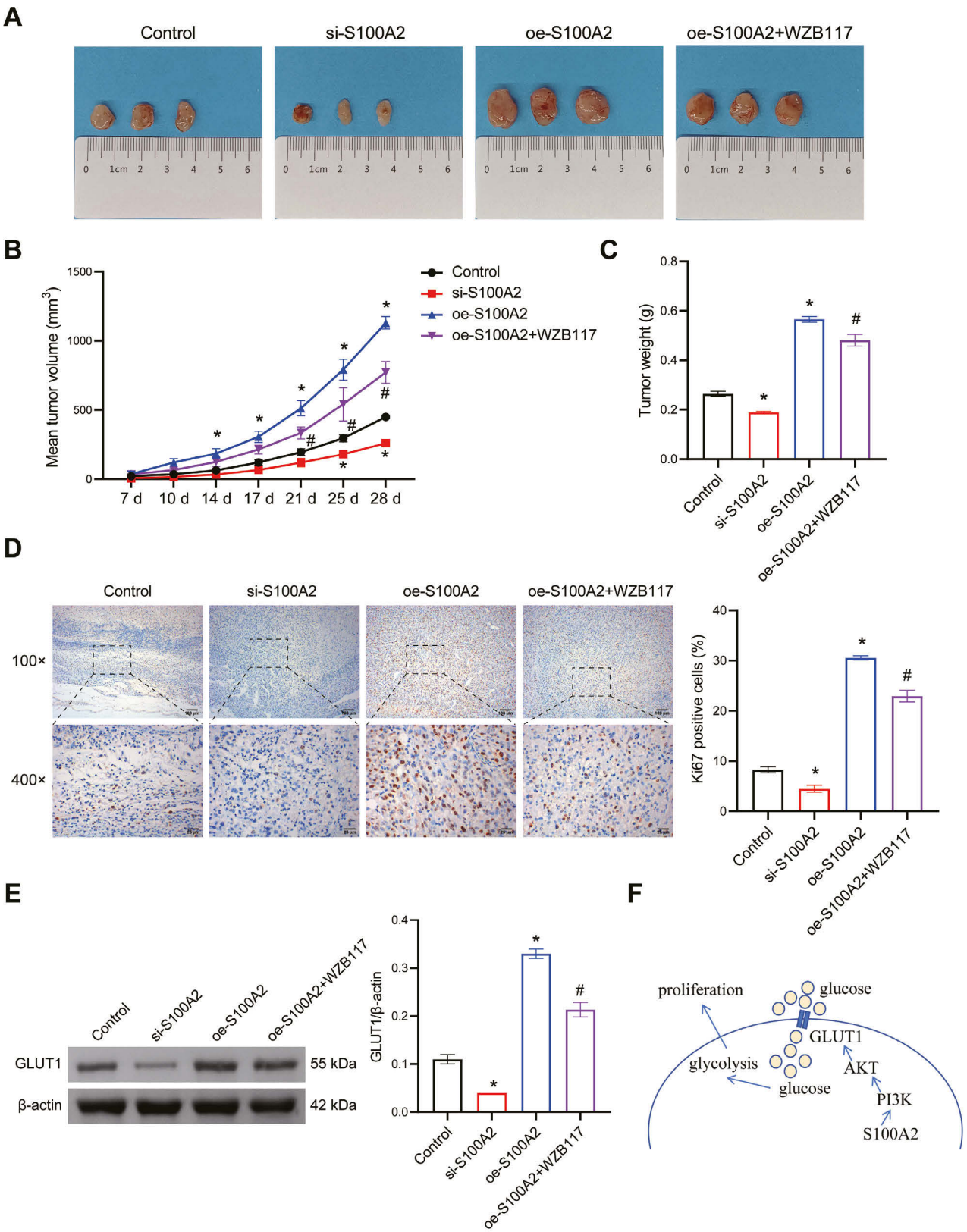

Fig. 9. S100A2 promoted NPC tumor formation by regulating GLUT1 expression. **A.** Tumor volume change curve from 7~28 days. **B.** Tumor observation at 28 days. **C.** Tumor weight at 28 days. **D.** Immunohistochemical detection of Ki-67 in tumor tissues (100 μm and 25 μm). **E.** GLUT1 expression in tumor tissues was detected by western blot. **F.** Diagram illustrating the relationships between S100A2, GLUT1, PI3K/ATK, proliferation, and glycolysis. N=3 mice/group. *p<0.05 vs. Control; $^{\#}p$<0.05 vs. oe-S100A2.

Recent findings from single-cell RNA sequencing have confirmed S100A2 as a potential biomarker of pancreatic adenocarcinoma (Zhao et al., 2021). Moreover, the specific inhibitor delanzomib, which targets the binding site of S100A2/KPNA2, has demonstrated the ability to inhibit the progression of colorectal cancer (Han et al., 2022). In a separate context, KDM5C has been shown to inhibit the expression of S100A2 through histone demethylation, leading to reduced migration and proliferation of thyroid papillary carcinoma cells (Wang et al., 2022). Our present study provides further evidence that silencing S100A2 not only inhibits the vitality, proliferation, glucose utilization, and lactate production of NPC cells, it also promotes apoptosis while downregulating the protein expression of GLUT1, HK2, and LDHA. These results underscore the potential of targeted inhibition of S100A2 as an effective approach to improve NPC treatment, although additional investigations are warranted to explore potential inhibitors of S100A2.

TET2 was reported to be underexpressed in NPC, and its overexpression inhibited glycolysis and the development of NPC through interaction with PKM (Zhang et al., 2020). High levels of S100A2 in gallbladder cancer promoted gallbladder carcinogenesis through the PI3K-Akt pathway (Dixit et al., 2022). This study demonstrates that overexpression of S100A2 promoted these characteristics and glycolysis in nasopharyngeal cancer cells but was blocked by LY294002. Then, due to limitations in experimental funding, we unperformed the experiments of si-S100A2 and LY294002 treatment in nasopharyngeal cancer cells. This was a limitation of our study. Results indicate that overexpression of S100A2 mediates the glycolysis process in nasopharyngeal cancer through the PI3K/AKT pathway, consistent with other studies.

Upregulation of SUMO2 promoted GLUT1 SUMOylation and ubiquitination, resulting in GLUT1 degradation, thereby inhibiting glycolysis and the malignant characteristics of NPC (Mo et al., 2021). The physical interaction between Epstein-Barr virus (EBV) latent membrane protein 1 (LMP1) and GLUT1 stabilized the GLUT1 protein by blocking its K48 ubiquitination and autophagic degradation, promoting aerobic glycolysis and immune escape in malignant cells (Cai et al., 2017). Loss of GLUT1 effectively inhibited aerobic glycolysis, cell proliferation, colony formation, and tumorigenic growth in LMP1-expressing nasopharyngeal epithelial (NPE) cells (Zhang et al., 2017). This study revealed that silencing S100A2 inhibited tumor formation and that overexpression of S100A2 promoted tumor formation but was blocked by a GLUT1 inhibitor (WZB117). These findings demonstrate that S100A2/GLUT1 inhibition suppresses tumor formation in NPC and may be an effective approach to inhibit EBV-associated subtypes of NPC, although further research is needed.

The interaction between S100A2 and p53 has been established as a viable drug target for pancreatic cancer (Sun et al., 2021). Additionally, S100A2 is closely associated with the immune status within the pancreatic cancer microenvironment and holds promise for predicting patient prognosis and immunotherapy response (Chen et al., 2021). Notably, S100A2 has been identified as a diagnostic biomarker of various malignancies, including non-small cell lung cancer patients with malignant pleural effusion, hepatocellular carcinoma, and prostate cancer (Cheng et al., 2021; Wang et al., 2021c; Yan et al., 2022). Furthermore, S100A2 has been recognized as a hypoxia-induced immunosuppressive factor that regulates PD-L1 expression, offering potential as a target for cervical cancer immunotherapy (Yang et al., 2024). These findings collectively establish S100A2 as a valuable prognostic marker and immunotherapeutic target for multiple cancers. While our study has provided preliminary evidence of S100A2's role in regulating glycolysis and tumor formation in NPC, its potential significance in clinical NPC prognosis and immunity remains uncharted territory. Given that there were only six cases of NPC patients in this study, it is still necessary to collect a large cohort of NPC samples to explore the diagnostic and immunotherapeutic value of S100A2 in NPC patients. Therefore, further investigations are warranted to explore the potential of S100A2 as a prognostic marker and immunotherapeutic target for NPC, which could potentially usher in new avenues of NPC treatment.

In summary, our findings reveal that S100A2 is significantly upregulated in the cancer tissues of NPC patients. Overexpression of S100A2 promotes both proliferation and glycolysis in NPC cells through the PI3K/AKT pathway. Importantly, our results indicate that GLUT1 can attenuate the impact of S100A2 on NPC tumor formation. Taken together, S100A2 and GLUT1 hold promise as potential targets for impeding the progression of NPC, especially in the context of EBV infection subtypes. Further research is warranted to explore the therapeutic implications of targeting the S100A2/GLUT1 axis in NPC.

Conflict of Interest. The authors declared that they have no conflicts of interest in this work.

Data availability statement. The data used to support the findings of this study are available from the corresponding author upon request.

Ethical statement. This study was approved by the Medical Ethics Committee of Changsha Central Hospital (No. 2021006). The research was conducted according to the World Medical Association Declaration of Helsinki. All the information about the study was fully explained to the subjects by the researchers. All participants provided informed consent before sampling.

All experimental procedures and animal handling were performed with the approval of the Animal Care and Use Committee of the Changsha Central Hospital (No. 2021006), which is affiliated with the University of South China, in accordance with the National Institutes of Health Guide for the Care and Use of Laboratory Animals, and studies involving laboratory animals follow the ARRIVE guidelines.

Funding Information. This study was supported by the scientific

research project funded by Hunan Provincial Health Commission (No. 202107011050).

Author contribution. Y.P. contributed to conceptualization, data curation, validation, and writing of the original draft. J.X. contributed to formal analysis and investigation. D.Z. contributed to software and validation. Z.Y. contributed to the methodology. R.Z. and M.X. contributed to investigation. H.P. contributed to conceptualization, funding acquisition, project administration, supervision, and review. All authors read and approved the final manuscript.

References

Cai T.T., Ye S.B., Liu Y.N., He J., Chen Q.Y., Mai H.Q., Zhang C.X., Cui J., Zhang X.S., Busson P., Zeng Y.X. and Li J. (2017). LMP1-mediated glycolysis induces myeloid-derived suppressor cell expansion in nasopharyngeal carcinoma. PLoS Pathog. 13, e1006503.

Cantù G. (2023). Nasopharyngeal carcinoma. A "different" head and neck tumour. Part A: from histology to staging. Acta Otorhinolaryngol. Ital. 43, 85-98.

Carrot-Zhang J., Chambwe N., Damrauer J.S., Knijnenburg T.A., Robertson A.G., Yau C., Zhou W., Berger A.C., Huang K.L., Newberg J.Y., Mashl R.J., Romanel A., Sayaman R.W., Demichelis F., Felau I., Frampton G.M., Han S., Hoadley K.A., Kemal A., Laird P.W., Lazar A.J., Le X., Oak N., Shen H., Wong C.K., Zenklusen J.C., Ziv E., Cherniack A.D. and Beroukhim R. (2020). Comprehensive analysis of genetic ancestry and its molecular correlates in cancer. Cancer Cell 37, 639-654.e6.

Chang E.T., Ye W., Zeng Y.X. and Adami H.O. (2021). The evolving epidemiology of nasopharyngeal carcinoma. Cancer Epidemiol. Biomarkers Prev. 30, 1035-1047.

Chen G., Sun W., Hua X., Zeng W. and Yang L. (2018). Long non-coding RNA FOXD2-AS1 aggravates nasopharyngeal carcinoma carcinogenesis by modulating miR-363-5p/S100A1 pathway. Gene 645, 76-84.

Chen Y., Wang C., Song J., Xu R., Ruze R. and Zhao Y. (2021). S100A2 is a prognostic biomarker involved in immune infiltration and predict immunotherapy response in pancreatic cancer. Front. Immunol. 12, 758004.

Cheng H., Wang Y., Liu C., Wu T., Chen S. and Chen M. (2021). Development and verification of a prostate cancer prognostic signature based on an immunogenomic landscape analysis. Front. Oncol. 11, 711258.

Ding R.B., Chen P., Rajendran B.K., Lyu X., Wang H., Bao J., Zeng J., Hao W., Sun H., Wong A.H., Valecha M.V., Yang E.J., Su S.M., Choi T.K., Liu S., Chan K.I., Yang L.L., Wu J., Miao K., Chen Q., Shim J.S., Xu X. and Deng C.X. (2021). Molecular landscape and subtype-specific therapeutic response of nasopharyngeal carcinoma revealed by integrative pharmacogenomics. Nat. Commun. 12, 3046.

Dixit R., Pandey M., Rajput M. and Shukla V.K. (2022). Unravelling of the comparative transcriptomic profile of Gallbladder cancer using mRNA sequencing. Mol. Biol. Rep. 49, 6395-6403.

Feng X., Zhang J., Chen W.N. and Ching C.B. (2011). Proteome profiling of Epstein-Barr virus infected nasopharyngeal carcinoma cell line: identification of potential biomarkers by comparative iTRAQ-coupled 2D LC/MS-MS analysis. J. Proteomics 74, 567-576.

Han F., Zhang L., Liao S., Zhang Y., Qian L., Hou F., Gong J., Lai M. and Zhang H. (2022). The interaction between S100A2 and KPNA2 mediates NFYA nuclear import and is a novel therapeutic target for colorectal cancer metastasis. Oncogene 41, 657-670.

Hu W., Tao Z., Zhou Q., Zhao D., Gu L., Zhu S. and Chen J. (2021). Effects of S100 calcium-binding protein A8 (S100A8) and S100 calcium-binding protein A9 (S100A9) on matrix metalloproteinase (MMP) expression in nasopharyngeal carcinoma CNE-2 cells. Transl. Cancer Res. 10, 1874-1884.

Huang F., Xiang X., Hong B., Min J. and Li J. (2019). Thyroid-like low-grade nasopharyngeal papillary adenocarcinoma. Am. J. Clin. Pathol. 152, 582-589.

Huang J., Fang J., Xu X., Qian X. and Zhang X. (2022). SETD1A promotes the proliferation and glycolysis of nasopharyngeal carcinoma cells by activating the PI3K/Akt pathway. Open Med. 17, 1849-1859.

Li A., Shi D., Xu B., Wang J., Tang Y.L., Xiao W., Shen G., Deng W. and Zhao C. (2017). S100A6 promotes cell proliferation in human nasopharyngeal carcinoma via the p38/MAPK signaling pathway. Mol. Carcinog. 56, 972-984.

Li C., Chen Q., Zhou Y., Niu Y., Wang X., Li X., Zheng H., Wei T., Zhao L. and Gao H. (2020). S100A2 promotes glycolysis and proliferation via GLUT1 regulation in colorectal cancer. FASEB J. 34, 13333-13344.

Lin S.J., Chang K.P., Hsu C.W., Chi L.M., Chien K.Y., Liang Y., Tsai M.H., Lin Y.T. and Yu J.S. (2013). Low-molecular-mass secretome profiling identifies C-C motif chemokine 5 as a potential plasma biomarker and therapeutic target for nasopharyngeal carcinoma. J. Proteomics 94, 186-201.

Lin Z., Deng L., Ji J., Cheng C., Wan X., Jiang R., Tang J., Zhuo H., Sun B. and Chen Y. (2016). S100A4 hypomethylation affects epithelial-mesenchymal transition partially induced by LMP2A in nasopharyngeal carcinoma. Mol. Carcinog. 55, 1467-1476.

Lin R., Bao X., Wang H., Zhu S., Liu Z., Chen Q., Ai K. and Shi B. (2021). TRPM2 promotes pancreatic cancer by PKC/MAPK pathway. Cell Death Dis. 12, 585.

Liu Y., Wang C., Shan X., Wu J., Liu H., Liu H., Zhang J., Xu W., Sha Z., He J. and Fan J. (2017). S100P is associated with proliferation and migration in nasopharyngeal carcinoma. Oncol. Lett. 14, 525-532.

Meng D.F., Sun R., Liu G.Y., Peng L.X., Zheng L.S., Xie P., Lin S.T., Mei Y., Qiang Y.Y., Li C.Z., Xu L., Peng X.S., Hu H., Lang Y.H., Liu Z.J., Wang M.D., Guo L.L., Xie D.H., Shu D.T., Li H.F., Luo F.F., Niu X.T., Huang B.J. and Qian C.N. (2020). S100A14 suppresses metastasis of nasopharyngeal carcinoma by inhibition of NF-κB signaling through degradation of IRAK1. Oncogene 39, 5307-5322.

Mo Y., Wang Y., Zhang S., Xiong F., Yan Q., Jiang X., Deng X., Wang Y., Fan C., Tang L., Zhang S., Gong Z., Wang F., Liao Q., Guo C., Li Y., Li X., Li G., Zeng Z. and Xiong W. (2021). Circular RNA circRNF13 inhibits proliferation and metastasis of nasopharyngeal carcinoma via SUMO2. Mol. Cancer 20, 112.

Oyang L., Ouyang L., Yang L., Lin J., Xia L., Tan S., Wu N., Han Y., Yang Y., Li J., Chen X., Tang Y., Su M., Luo X., Li J., Xiong W., Zeng Z., Liao Q. and Zhou Y. (2023). LPLUNC1 reduces glycolysis in nasopharyngeal carcinoma cells through the PHB1-p53/c-Myc axis. Cancer Sci. 114, 870-884.

Shibuya K., Okada M., Suzuki S., Seino M., Seino S., Takeda H. and Kitanaka C. (2015). Targeting the facilitative glucose transporter GLUT1 inhibits the self-renewal and tumor-initiating capacity of cancer stem cells. Oncotarget 6, 651-661.

Sugino H. and Sawada Y. (2022). Influence of S100A2 in human diseases. Diagnostics 12, 1756.

Sun J., Ambrus J.I., Russell C.C., Baker J.R., Cossar P.J., Pirinen M.J., Sakoff J.A., Scarlett C.J. and McCluskey A. (2021). Targeting the S100A2-p53 interaction with a series of 3,5-Bis(trifluoromethyl)benzene sulfonamides: Synthesis and cytotoxicity. ChemMedChem. 16, 2851-2863.

Tang L.L., Chen Y.P., Chen C.B., Chen M.Y., Chen N.Y., Chen X.Z., Du X.J., Fang W.F., Feng M., Gao J., Han F., He X., Hu C.S., Hu D.S., Hu G.Y., Jiang H., Jiang W., Jin F., Lang J.Y., Li J.G., Lin S.J., Liu X., Liu Q.F., Ma L., Mai H.Q., Qin J.Y., Shen L.F., Sun Y., Wang P.G., Wang R.S., Wang R.Z., Wang X.S., Wang Y., Wu H., Xia Y.F., Xiao S.W., Yang K.Y., Yi J.L., Zhu X.D. and Ma J. (2021). The Chinese Society of Clinical Oncology (CSCO) clinical guidelines for the diagnosis and treatment of nasopharyngeal carcinoma. Cancer Commun. 41, 1195-1227.

Tang L.L., Guo R., Zhang N., Deng B., Chen L., Cheng Z.B., Huang J., Hu W.H., Huang S.H., Luo W.J., Liang J.H., Zheng Y.M., Zhang F., Mao Y.P., Li W.F., Zhou G.Q., Liu X., Chen Y.P., Xu C., Lin L., Liu Q., Du X.J., Zhang Y., Sun Y. and Ma J. (2022). Effect of radiotherapy alone vs radiotherapy with concurrent chemoradiotherapy on survival without disease relapse in patients with low-risk nasopharyngeal carcinoma: A randomized clinical trial. JAMA 328, 728-736.

Wang C., Wang X., Han A., Wang Y. and Jiang H. (2021a). Proof-of-concept study investigating the role of S100P-RAGE in nasopharyngeal carcinoma. Exp. Ther. Med. 21, 470.

Wang T., Du G. and Wang D. (2021b). The S100 protein family in lung cancer. Clin. Chim. Acta 520, 67-70.

Wang T., Wang N., Zhang L., Liu Y. and Thakur A. (2021c). S100A2: A potential biomarker to differentiate malignant from tuberculous pleural effusion. Indian J. Cancer 58, 241-247.

Wang Y., Ye H., Yang Y., Li J., Cen A. and Zhao L. (2022). microRNA-181a promotes the oncogene S100A2 and enhances papillary thyroid carcinoma growth by mediating the expression of histone demethylase KDM5C. J. Endocrinol. Invest. 45, 17-28.

Yan L.L., Huang Y.J., Yi X., Yan X.M., Cai Y., He Q. and Han Z.J. (2015). Effects of silencing S100A8 and S100A9 with small interfering RNA on the migration of CNE1 nasopharyngeal carcinoma cells. Oncol. Lett. 9, 2534-2540.

Yan J., Huang Y.J., Huang Q.Y., Liu P.X. and Wang C.S. (2022). Transcriptional activation of S100A2 expression by HIF-1α via binding to the hypomethylated hypoxia response elements in HCC cells. Mol. Carcinog. 61, 494-507.

Yang Y., Zeng Z., Li L., Lei S., Wu Y., Chen T. and Zhang J. (2023). Sinapine thiocyanate exhibited anti-colorectal cancer effects by inhibiting KRT6A/S100A2 axis. Cancer Biol. Ther. 24, 2249170.

Yang J., Wan S., Zhao M., Cai H., Gao Y. and Wang H. (2024). Multi-omics analysis identifies hypoxia subtypes and S100A2 as an immunosuppressive factor in cervical cancer. Reprod. Sci. 31, 107-121.

Zhang J., Jia L., Lin W., Yip Y.L., Lo K.W., Lau V.M.Y., Zhu D., Tsang C.M., Zhou Y., Deng W., Lung H.L., Lung M.L., Cheung L.M. and Tsao S.W. (2017). Epstein-barr virus-encoded latent membrane protein 1 upregulates glucose transporter 1 transcription via the mTORC1/NF-κB signaling pathways. J. Virol. 91, e02168-16.

Zhang X., Yang J., Shi D. and Cao Z. (2020). TET2 suppresses nasopharyngeal carcinoma progression by inhibiting glycolysis metabolism. Cancer Cell Int. 20, 363.

Zhang Q., Xia T., Qi C., Du J. and Ye C. (2022). High expression of S100A2 predicts poor prognosis in patients with endometrial carcinoma. BMC Cancer 22, 77.

Zhao X., Li H., Lyu S., Zhai J., Ji Z., Zhang Z., Zhang X., Liu Z., Wang H., Xu J., Fan H., Kou J., Li L., Lang R. and He Q. (2021). Single-cell transcriptomics reveals heterogeneous progression and EGFR activation in pancreatic adenosquamous carcinoma. Int. J. Biol. Sci. 17, 2590-2605.

Zhou J.C., Zhang J.J., Zhang W., Ke Z.Y., Ma L.G. and Liu M. (2017). Expression of GLUT-1 in nasopharyngeal carcinoma and its clinical significance. Eur. Rev. Med. Pharmacol. Sci. 21, 4891-4895.

Accepted June 11, 2024